Anomalous Isotopic Effect Near the Charge-Ordering Quantum Criticality

S. Andergassen, S. Caprara, C. Di Castro, and M. Grilli

Istituto Nazionale per la Fisica della Materia, Unità di Roma 1,

and Dipartimento di Fisica, Università di Roma "La Sapienza," Piazzale Aldo Moro 2, I-00185 Roma, Italy

Within the Hubbard-Holstein model, we evaluate the crossover lines marking the opening of pseudogaps in the cuprates, which, in our scenario, are ruled by the proximity to a charge-ordering quantum criticality (stripe formation). We find that their isotopic dependence, due to critical fluctuations, implies a substantial positive shift of the pseudogap-formation temperature T^*. We infer that the isotopic shift of the superconducting T_c is nearly absent in the optimally and overdoped regimes and is negative and increasing upon underdoping. The dynamical nature of the charge-ordering transition may explain the spread of the experimental values of T^*.

There is much experimental evidence [1] that the peculiar properties of the cuprates, both in the normal and in the superconducting phase, are controlled by a quantum critical point (QCP), located near the optimal doping $\delta = \delta_{\mathrm{opt}}$. In this framework the phase diagram of the cuprates is naturally partitioned into a (nearly) ordered, a quantum critical, and a quantum disordered region corresponding to the underdoped, optimally, and overdoped regions, respectively. The ordered region occurs below a second-order transition line $T_?(\delta)$, which depends on the nature of the underlying ordering and, upon increasing δ, ends at $T = 0$ in a QCP (at $\delta = \delta_c \gtrsim \delta_{\mathrm{opt}}$). This correspondence leads to a close connection [1] between the hypothetical $T_?(\delta)$ and the crossover line $T^*(\delta)$, below which a pseudogap behavior is observed in nuclear quadrupole resonance (NQR), nuclear magnetic resonance (NMR), x-ray absorption near-edge structure, and angle-resolved photoemission spectroscopy measurements [see, e.g., Ref. [2] for a recent overview on La$_{2-\delta}$Sr$_\delta$CuO$_4$ (LSCO)]. In the proximity of quantum criticality, critical fluctuations mediate a singular interaction among the quasiparticles which can account for both the violation of the Fermi-liquid behavior observed in the normal phase of the cuprates, and the strong pairing mechanism leading to high-T_c superconductivity [1,3–5]. Various realizations of this scenario have been proposed, associated with different quantum criticalities, e.g., antiferromagnetic [3], excitonic [4], change in the symmetry of the superconducting order parameter [6], or incommensurate charge-density wave [5].

In the QCP framework, any mechanism shifting the position of the QCP is mirrored by corresponding shifts in $T_?(\delta)$ and in the superconducting critical line $T_c(\delta)$. In particular, the observation of isotopic effects (IE's) on T_c [7,8] and on T^* [9–11] suggests that a lattice mechanism underlies the instability marked by the QCP. We here consider the single-band Hubbard-Holstein model with long-range Coulomb forces as a minimal model to describe the strongly correlated electrons coupled to the lattice, giving rise to a QCP for the onset of a phonon-induced incommensurate charge ordering (CO) [5,12,13]. This introduces density inhomogeneities on a semimicroscopic scale and corresponds to the onset of stripes [14], coming from the high-doping regime. Thus, in our approach, the critical line $T_?(\delta)$ corresponds to the line for CO, $T_{\mathrm{CO}}(\delta)$, which in real materials can be masked by pair formation and lattice effects.

In this Letter, we first determine the mean-field (mf) critical line $T_{\mathrm{CO}}^{(0)}(\delta)$, which we identify with the weak-pseudogap crossover line $T^0(\delta)$ $[\gg T^*(\delta)]$ observed in Knight-shift, transport, and static susceptibility measurements [2], as the incipient depression of the single-particle density of states (DOS). Indeed, for $T < T_{\mathrm{CO}}^{(0)}$ one expects the CO fluctuations to become substantial, leading to a reduction of the quasiparticle DOS. Then, we investigate the effect of fluctuations near the CO QCP in order to determine (a) the fluctuation-corrected critical line $T_{\mathrm{CO}}(\delta)$, which we relate to the pseudogap crossover line $T^*(\delta)$; (b) the IE on $T_{\mathrm{CO}}(\delta)$, from which we also infer the effect on $T_c(\delta)$. In particular, we describe the highly nontrivial effect of quantum criticality in determining IE's on T^* and T_c, which can be strong and weak, respectively, and opposite in sign in the underdoped cuprates. We also show why both T^* and its isotopic shift are observed to be larger in experiments with shorter characteristic time scales. The near absence of IE on T_c near and above δ_{opt} is also accounted for naturally.

The model and the mean-field instability.—Our two-dimensional (2D) Hamiltonian is

$$
\begin{aligned}
H = &-t \sum_{\langle i,j\rangle,\sigma} (c_{i\sigma}^\dagger c_{j\sigma} + \mathrm{H.c.}) - t' \sum_{\langle\langle i,j\rangle\rangle,\sigma} (c_{i\sigma}^\dagger c_{j\sigma} + \mathrm{H.c.}) \\
&- \mu_0 \sum_{i\sigma} n_{i\sigma} + U \sum_i n_{i\uparrow} n_{i\downarrow} + \frac{1}{2} \sum_{\mathbf{q}\neq 0} V_C(\mathbf{q}) \rho_{\mathbf{q}} \rho_{-\mathbf{q}} \\
&+ \omega_0 \sum_i a_i^\dagger a_i + g \sum_{i,\sigma} (a_i^\dagger + a_i)(n_{i\sigma} - \langle n_{i\sigma}\rangle),
\end{aligned}
\tag{1}
$$

where $c_{i\sigma}^{(\dagger)}$ are the fermion operators, $a_i^{(\dagger)}$ are the phonon operators, $\langle i,j\rangle$ and $\langle\langle i,j\rangle\rangle$ indicate nearest- and next-nearest-neighbor sites, coupled by the hopping parameters t and t', respectively. The lattice spacing has been set to unity. The chemical potential μ_0 is coupled to the local electron density $n_{i\sigma} \equiv c_{i\sigma}^{\dagger}c_{i\sigma}$, U is the on-site Hubbard repulsion, and $\rho_{\mathbf{q}} \equiv \sum_{\mathbf{k},\sigma} c_{\mathbf{k+q},\sigma}^{\dagger}c_{\mathbf{k},\sigma}$. $V_C(\mathbf{q})$ ($\approx V_C/|\mathbf{q}|$ at small $|\mathbf{q}|$) is the Coulomb interaction between electrons in a 2D plane embedded in the three-dimensional (3D) space [5,13]. ω_0 is the phonon frequency and g is the Holstein electron-phonon coupling. In the limit $U \rightarrow \infty$, this model was solved with a standard slave-boson technique, at leading order within a large-N expansion in Refs. [5,13]. The most relevant result was that a CO instability with a finite wave vector $\mathbf{q}_c$, incommensurate with the underlying lattice, was found at $T = 0$ when δ is reduced below a critical value $\delta_c^{(0)}$. Besides a small, weakly momentum-dependent, residual repulsion, nearby this instability the critical charge fluctuations mediate a singular scattering

$$\Gamma(\mathbf{q},\omega_n) \approx -\frac{V}{\xi_0^{-2} + |\mathbf{q} - \mathbf{q}_c|^2 + \gamma|\omega_n|} \qquad (2)$$

of strength V, between the quasiparticles. Here ω_n is a bosonic Matsubara frequency, $\gamma \sim t^{-1}$ is a characteristic time scale, and ξ_0^{-2} is the mf inverse square correlation length, which measures the distance from criticality. Equation (2) displays the behavior of a Gaussian QCP with a dynamical critical index $z = 2$.

Quite remarkably, the complicated formal structure of the quasiparticle scattering, mediated by slave bosons, phonons, and by the Coulomb interaction, is well represented near criticality by a RPA resummation $\Gamma(\mathbf{q},\omega_n) \approx V_{\text{eff}}(\mathbf{q})/[1 + V_{\text{eff}}(\mathbf{q})\Pi(\mathbf{q},\omega_n)]$ of an effective static interaction $V_{\text{eff}}(\mathbf{q}) = \tilde{U}(\mathbf{q}) + V_C(\mathbf{q}) - \lambda t$ [15]. Here Π is the fermionic polarization bubble in a 2D lattice, $\lambda \equiv 2g^2/t\omega_0$ is the dimensionless electron-phonon coupling, and $\tilde{U}(\mathbf{q}) \simeq A + B|\mathbf{q}|^2$ is the residual short-range repulsion between quasiparticles. For the correspondence of $V_{\text{eff}}(\mathbf{q})$ with the parameters of Eq. (1), see Ref. [15]. The instability condition, which occurs for reasonable values $\lambda \sim 1$, is $1 + V_{\text{eff}}(\mathbf{q}_c)\Pi(\mathbf{q}_c, \omega = 0) = 0$. At $T = 0$ this determines $\mathbf{q}_c$ and the position of the mf QCP $\delta_c^{(0)}$. For realistic parameters we find $\mathbf{q}_c \approx (\pm 1, 0)$ or $(0, \pm 1)$, and $\delta_c^{(0)} \approx 0.2$ [5,13]. By expanding $1 + V_{\text{eff}}\Pi$ near the instability at $T = 0$, we find $\xi_0^{-2} \propto \delta - \delta_c^{(0)}$, which gives the Gaussian index $\nu = 1/2$ for ξ_0. The mf critical line $T_{\text{CO}}^{(0)}(\delta)$ (the solid-line curve in Fig. 1), which starts from the mf QCP at $\delta_c^{(0)}$ is obtained by considering the T dependence of the bare polarization bubble, which reduces to the simple Fermi-liquid form, $\propto T^2$, at low T. We identify this mf transition with the experimental crossover line T^0, extrapolating to low T at a doping, which we identify with our $\delta_c^{(0)}$. From the data reported in Ref. [2], for LSCO we estimate $\delta_c^{(0)} \approx 0.22$. Then we evaluate $T_{\text{CO}}^{(0)}(\delta)$ by taking
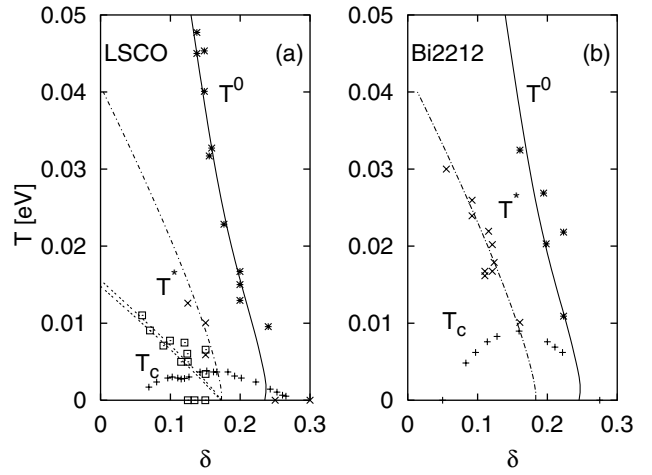
FIG. 1. The phase diagram of the cuprates according to the CO-QCP scenario for LSCO (a) and Bi2212 (b). The solid line is the mf critical line ending at $T = 0$ in the mf QCP at $\delta_c^{(0)}$. The lowest dashed line in panel (a) marks the 3D critical line in the presence of fluctuations, ending in the QCP at δ_c. We took $\Omega_\perp = 1$ meV (see text). The dot-dashed line in panels (a),(b) indicates the "dynamical instability" condition (see text) for $\omega_{\text{probe}} = 1$ meV. The intermediate dashed line in panel (a) represents the dynamical instability condition for $\omega_{\text{probe}} = 1$ μeV. The experimental points for T^0 (*) and for T^* measured with fast (×) and slow (□) probes for LSCO are from Ref. [2]; those for Bi2212 are from Refs. [16,17]. The experimental critical temperatures T_c are also shown (+).

standard quasiparticle (i.e., dressed by the slave bosons) band parameters ($t_{\text{qp}} = 0.2$ eV, $t'_{\text{qp}} = -0.05$ eV, $\omega_0 = 0.07$ eV, leading to $A = 0.2$ eV and $B = 0.17$ eV in the residual repulsion $\tilde{U}$). $V_C = 0.22$ eV and $g = 0.21$ eV are adjusted to match the experimental extrapolation of T^0 with the $T = 0$ mf instability (i.e., $\delta_c^{(0)}$). We point out that the agreement between $T_{\text{CO}}^{(0)}(\delta)$ and $T^0(\delta)$ at finite T is obtained without any further adjustment of the parameters. Similar parameters are taken for $Bi_2Sr_2CaCu_2O_8$ (Bi2212) to fit the data in Refs. [16,17], with $V_C = 0.22$ eV and $g = 0.23$ eV.

The phase diagram beyond mean field.—The fluctuations shift the mf QCP and critical line to their actual position [18,19]. Specifically the fluctuations which mediate the effective critical interaction, Eq. (2), can be included in the polarization bubble via the diagrams of Fig. 2a, leading to corrections beyond RPA. From the explicit evaluation of these diagrams we find the (self-consistent) correction to the mass term $m \equiv \gamma^{-1}\xi^{-2}$ of the fluctuation propagator, Eq. (2),

$$m = m_0 + 12uT \sum_{|\omega_n|<\omega_0} \sum_{\mathbf{q}} D(\mathbf{q},\omega_n;m), \qquad (3)$$

where $D = (\Omega_{\mathbf{q}} + |\omega_n|)^{-1}$ is the charge-fluctuation critical propagator and $u \sim V^2/(\gamma^2 t^3)$ is the coupling resulting from the two four-leg vertices represented in Fig. 2b. The critical modes have a 2D dispersion $\Omega_{\mathbf{q}} = \gamma^{-1}|\mathbf{q} - \mathbf{q}_c|^2 + m$, up to an ultraviolet bandwidth cutoff $\Omega_{\text{max}} \sim \gamma^{-1}$, resulting from the underlying lattice. Since we deal
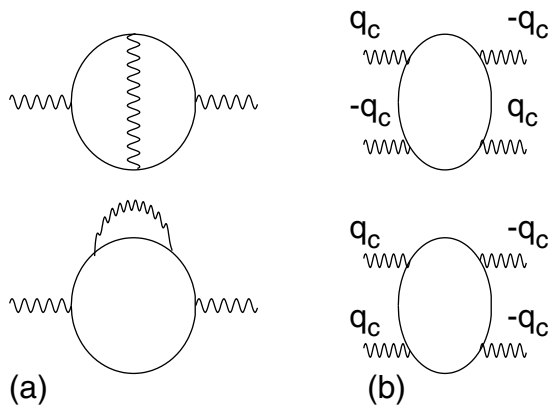
FIG. 2. (a) The two (vertex and self-energy) corrections to the fermionic bubbles (solid line) due to critical charge fluctuations (wavy line). (b) Effective four-leg vertices for the critical charge fluctuation field (wavy line) resulting from the integration over the fermion loops (solid line).

with a phonon-driven CO instability, as it also follows from the detailed dynamical analysis of Ref. [13], ω_0 appears as the ultraviolet frequency cutoff. By introducing the DOS $N(\Omega) = \sum_{\mathbf{q}} \delta(\Omega - \Omega_{\mathbf{q}})$ and the spectral-density representation of D, we rewrite Eq. (3) in the form

$$m = m_0 + \frac{24u}{\pi} \int_m^{\Omega_{max}} d\Omega \, N(\Omega) \int_0^\infty dz \, \frac{z}{z^2 + \Omega^2}$$
$$\times \left[b(z) + \frac{1}{2} - \frac{1}{\pi} \arctan \frac{z}{\omega_0} \right], \qquad (4)$$

where $b(z) = [\exp(z/T) - 1]^{-1}$. At $T = 0$, Eq. (4) with $m = 0$ leads to a finite shift of the 2D QCP $\delta_c^{(0)} - \delta_c \propto \omega_0$ (see Fig. 1). At finite T, as a consequence of a constant DOS for the 2D modes, the integral in Eq. (4) is logarithmically divergent for $m \to 0$, leading to a vanishing of the renormalized T_{CO} (Mermin-Wagner theorem). This divergency is removed by considering the more realistic anisotropic 3D character of the critical fluctuations, introducing a small energy scale $\Omega_\perp$, below which the mode DOS is no longer constant, and displays a 3D square-root behavior $N(\Omega < \Omega_\perp) \sim \sqrt{\Omega}$ at criticality. This is enough to make the integral in Eq. (4) convergent and allows one to determine the critical line [Eq. (4) with $m = 0$] in the anisotropic 3D case as reported in Fig. 1a (lowest dashed line). The inclusion of fluctuations brings the critical line from temperatures of the order of typical electronic energies ($T_{CO}^{(0)} \sim t$) down to much lower temperatures T_{CO} of the order of the observed T^*'s. Indeed, within the CO-QCP scenario, the pseudogap arises at $T < T^*$ because the quasiparticles feel an increasingly strong interaction by approaching the critical line $T_{CO}(\delta)$. In the particle-hole channel, this interaction can produce a gap due to the incipient CO. At the same time in the particle-particle channel, the strong attraction can lead to pair formation even in the absence

of phase coherence. Therefore $T^*(\delta)$ closely tracks the underlying transition line $T_{CO}(\delta)$.

On the other hand, the spread in the measured values of T^* depending on the experimental probe (see, e.g., Ref. [2]) indicates that the CO instability may be "dynamical," $\Omega_\perp$ being smaller than (or comparable to) typical frequencies of the experimental probes, ω_{probe}. In this case the self-consistency condition (4) includes ω_{probe} as the infrared cutoff in the integral over Ω, m being replaced by ω_{probe}. This determines the doping and temperature dependence of the dynamical instability lines. Two examples are reported in Fig. 1 for $\omega_{probe} = 1$ meV (dot-dashed line if Figs. 1a and 1b), as in typical neutron scattering experiments, and $\omega_{probe} = 1$ μeV (second dashed line from bottom in Fig. 1a), as in static experiments (NQR, NMR). The corresponding experimental data for T^* in LSCO are also reported for comparison. We determine the coupling V between the charge fluctuations and the quasiparticles, which is the only parameter for which an *a priori* estimate is difficult, by imposing that the fluctuation-corrected QCP is located at the $T = 0$ extrapolation of the $T^*(\delta)$ curves. We used $\gamma = 0.7$ eV^{-1} and $\gamma = 0.4$ eV^{-1} for LSCO and Bi2212, respectively, and $V = 0.54$ eV for both. It is worth noticing that, similarly to the case of $T_{CO}^{(0)}(\delta)$, the agreement between the calculated $T_{CO}(\delta)$ and the experimental $T^*(\delta)$ is obtained without further adjustable parameters. We also notice that, contrary to the shift of δ_c at $T = 0$, the slope of $T_{CO}(\delta)$ is weakly dependent on ω_0.

Novel isotopic effects.—The mf weak-pseudogap crossover temperature $T_{CO}^{(0)} \sim T^0$ is determined by λ only. Therefore, it does not depend on ω_0 and is *not* expected to display any isotopic dependence. On the other hand, quantities determined by the fluctuations crucially involve ω_0. New physical effects can then arise in the isotopic substitutions. Since ω_0 decreases by increasing the ionic mass, the corrections to $\delta_c^{(0)}$ and to $T_{CO}^{(0)}(\delta)$ become smaller and the fluctuation-corrected quantities δ_c and T_{CO} shift to higher doping, closer to the mf values, as shown in Fig. 3, where we report the line $T_{CO}(\delta)$, calculated via Eq. (4), with parameters to fit the T^* data of LSCO (see above), together with its isotopic shift calculated for ^{16}O $\to$ ^{18}O substitution (i.e., for a 5% reduction of ω_0). Correspondingly we expect that the portion of the curve $T_c(\delta)$ on the left of $T^0(\delta)$ is rigidly translated along the horizontal axis. The rationale behind this translation is that the whole physics of these materials is essentially determined by the proximity to the critical line $T_{CO}(\delta)$ and to the related QCP. On the other hand, on the right of the mf critical line $T_{CO}^{(0)}(\delta) \sim T^0(\delta)$ the fluctuations are small and the physical processes at $T > T^0(\delta)$ are captured by the mf description, where λ (not ω_0) is relevant. As a consequence $T^0(\delta)$ and the portion of $T_c(\delta)$ near and above $T^0(\delta)$ are not expected to be shifted by IE's.

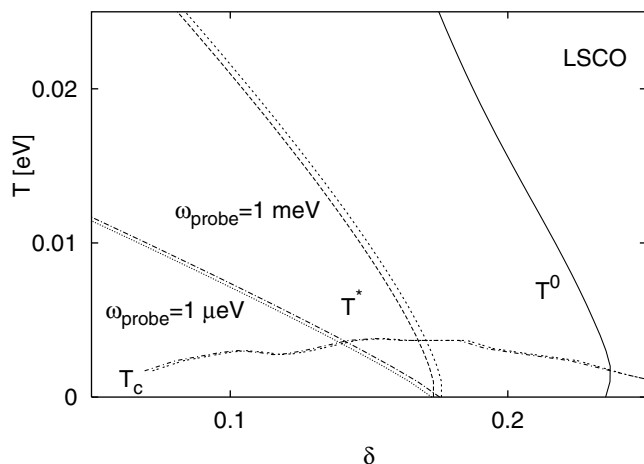In the underdoped region, there are two evident consequences of the isotopic shift, which becomes more

FIG. 3. Calculated effect of the isotopic change $^{16}O \rightarrow {}^{18}O$ (i.e., $\omega_0 = 70$ meV and $\omega_0' = 66$ meV) on T^* in LSCO, both for a fast- and a slow-probe measurement. The inferred shift on T_c is also reported.

substantial: The shift upon reducing ω_0 is negative (as usual) in T_c, but, contrary to standard theories based on CO pseudogap [20], it is *positive* in $T_{CO} \sim T^*$. Moreover, when the slope of $T_{CO}(\delta)$ is large, a rather small isotopic shift in δ_c can result in a substantial shift in $T_{CO} \sim T^*$. The steeper T^* is, the larger the IE is. On the other hand, since the curve $T_c(\delta)$ is rather flat, particularly in the optimal and moderately underdoped regimes, the expected IE on T_c in these compounds is small in agreement with long-standing experiments [7,8]. This large difference in the IE for T_c and T^*, $(\Delta T_c/\Delta M)/(\Delta T^*/\Delta M) \ll 1$, is indeed experimentally observed in $HoBa_2Cu_4O_8$ (HBCO-124), and reported in Ref. [11], where it is also noticed that there is a "striking similarity between isotopic substitution and underdoping with respect to both T_c and T^*." Although we are not aware of any systematic analysis of the doping dependencies of T_c, T^* and their isotopic shifts in HBCO-124, this observation finds its natural interpretation within our QCP scenario, where the isotopic substitution produces a shift of the QCP and is therefore nearly equivalent to underdoping.

The slope of $T_{CO}(\delta)$ increases by increasing ω_{probe}, while the QCP is unshifted. Therefore, the IE on $T_{CO} \sim T^*$ is enhanced, and we have the general trend that faster probes should detect a larger IE on T^*, since the effect of fluctuation diminishes. Although we cannot account for the near-absent or negative IE on T^* within the almost static probes in $YBa_2Cu_4O_8$ [9,10], this general trend is in qualitative agreement with a much stronger effect observed in the isostructural HBCO-124 with fast neutron scattering [11]. Indeed, this fast-probe experiment should be represented by the curve $T_{CO}(\delta)$ corresponding to $\omega_{probe} = 1$ meV in Fig. 3. The huge IE on T^* observed in HBCO-124 suggests that the curve $T_{CO}(\delta)$ in this system is steeper than in LSCO.

Upon underdoping, while T_c decreases, its IE increses in agreement with a general experimental trend [7]. However, in the strongly underdoped materials, where a substantial IE in the penetration depth [21] and in the x-ray absorption [22] have been observed, our results can provide only qualitative indications, as other effects (magnetic, polaronic, lattice pinning) not included in (1) become relevant. For this doping regime, a different (additional) interpretation of the IE in terms of a superconductor-to-insulator QCP has been recently proposed [23].

[1] For a summary of this evidence, see, e.g., the introduction of C. Castellani, C. Di Castro, and M. Grilli, Z. Phys. **103**, 137 (1997); J. L. Tallon and J. W. Loram, Physica (Amsterdam) **349C**, 53 (2001).
[2] M. Gutmann, E. S. Božin, and S. J. L. Billinge, cond-mat/0009141.
[3] A. J. Millis, H. Monien, and D. Pines, Phys. Rev. B **42**, 167 (1990); S. Sachdev and J. Ye, Phys. Rev. Lett. **69**, 2411 (1992).
[4] C. M. Varma, Phys. Rev. Lett. **83**, 3538 (1999).
[5] C. Castellani, C. Di Castro, and M. Grilli, Phys. Rev. Lett. **75**, 4650 (1995).
[6] M. Vojta, Y. Zhang, and S. Sachdev, Phys. Rev. Lett. **85**, 4940 (2000).
[7] J. P. Franck, in *Physical Properties of High Temperature Superconductors IV*, edited by D. M. Ginsberg (World Scientific, Singapore, 1994), p. 189.
[8] M. K. Crawford *et al.,* Phys. Rev. B **41**, 282 (1990).
[9] F. Raffa *et al.,* Phys. Rev. Lett. **81**, 5912 (1998).
[10] G. V. M. Williams *et al.,* Phys. Rev. B **61**, R9257 (2000).
[11] D. Rubio Temprano *et al.,* Phys. Rev. Lett. **84**, 1990 (2000).
[12] A. Perali *et al.,* Phys. Rev. B **54**, 16 216 (1996).
[13] F. Becca *et al.,* Phys. Rev. B **54**, 12 443 (1996).
[14] In our framework the CO instability is a second-order transition leading to a gradual increase of the charge modulation. It is only when one enters deeply inside the (locally) ordered phase that anharmonic distortions of the charge profile may arise from the enhanced interactions with the spin and the lattice degrees of freedom. This may lead to the stripe formation, as revealed in neutron scattering; see J. M. Tranquada *et al.,* Nature (London) **375**, 561 (1995).
[15] G. Seibold *et al.,* Eur. Phys. J. B **13**, 87 (2000).
[16] H. Ding *et al.,* J. Phys. Chem. Solids **59**, 1888 (1998).
[17] K. Ishida *et al.,* Phys. Rev. B **58**, R5960 (1998).
[18] J. A. Hertz, Phys. Rev. B **14**, 1165 (1976).
[19] A. J. Millis, Phys. Rev. B **48**, 7183 (1993).
[20] R. S. Markiewicz, Physica (Amsterdam) **169C**, 63 (1990); I. Eremin *et al.,* Phys. Rev. B **56**, 11 305 (1997).
[21] J. Hofer *et al.,* Phys. Rev. Lett. **84**, 4192 (2000).
[22] A. Lanzara *et al.,* J. Phys. Condens. Matter **11**, L541 (1999).
[23] T. Schneider and H. Keller, cond-mat/0011381.